Desalination and Water Treatment
www.deswater.com

doi: 10.5004/dwt.2018.21684

102 (2018) 151–164
January

Preparation and performance analysis of chitosan/polyacrylamide/poly (vinyl alcohol)/Fe/glutaraldehyde copolymer for Cr(VI) adsorption

Xu Xin[a], Yaoguo Wu[a,*], Sihai Hu[a,b], Yuanjing Zhang[a,b]

[a]*Department of Applied Chemistry, Northwestern Polytechnical University, Xi'an 710129, China, Tel. +86-88431672, emails: wuygal@nwpu.edu.cn (Y. Wu), 2350084479@qq.com (X. Xin), hsh18621@163.com (S. Hu), mirror2yj@163.com (Y. Zhang)*
[b]*Key Laboratory of Groundwater Contamination and Remediation, China Geological Survey (CGS) & Hebei Province, Shijiazhuang 050000, China*

Received 6 March 2017; Accepted 17 November 2017

ABSTRACT

In this study, chitosan/polyacrylamide/poly(vinyl alcohol)/Fe/glutaraldehyde (CPPFG) copolymers, termed as CPPFG I, II, III and IV, respectively, were prepared with corresponding amounts of glutaraldehyde (GA). These copolymers were then employed to do batch experiments as a function of pH, Cr(VI) initial concentration, contact time, temperature and coexisting anions to study Cr(VI) adsorption process. Scanning electron microscopy (SEM), Fourier transform infrared spectroscopy (FTIR) and X-ray photoelectron spectroscopy (XPS) were used to explore the characteristics of the adsorbents before and after loaded Cr(VI) and adsorption mechanism. The results showed that the copolymers had a fast adsorption rate and high adsorption efficiency above 99.50% which was hardly affected by initial pH values varying from 3.0 to 8.0 and the anions. The adsorption fitted Langmuir and Temkin isotherm models well. The removal of Cr(VI) followed pseudo-second-order and intraparticle diffusion kinetic models, and its rate was mainly controlled by chemical adsorption and intraparticle mass transport. The calculated thermodynamic parameters (ΔG^0, ΔH^0 and ΔS^0) demonstrated that the adsorption was a spontaneous and endothermic process. The adsorption capacity and rate were strongly depended on the quantity of the available functional binding sites (i.e., –OH, –C=N and –NH), and surface morphologies with different GA cross-link densities under the studied conditions. The possible mechanism was proposed based on the data of FTIR, XPS, SEM and zeta potential. Adsorption properties comparison showed the copolymer was an alternative as adsorbent to remove Cr(VI) from natural water.

Keywords: Hexavalent chromium (Cr(VI)); Copolymer; Preparation; Adsorption; Water treatment

1. Introduction

Chromium (Cr) is not only a common contaminant in industrial wastewater, deriving from electroplating, leather tanning and textile activities [1,2], but also presents in natural water including surface water and groundwater [3]. Cr is mainly in two stable oxidation states, the trivalent and hexavalent chromium (Cr(III) and Cr(VI)) [4,5]. Cr(III) is a micronutrient with relatively low toxicity, whereas Cr(VI) is a known carcinogen and irritant through inhalation and a potential health hazard through ingestion [6]. The United States Environmental Protection Agency sets the maximum contaminant level for total chromium in drinking water 100 μg L^{-1}, and the World Health Organization even sets a much strict threshold 50 μg L^{-1} [7,8]. Hence, considerable interest has been focused on searching methods to remove Cr(VI) from water, such as chemical precipitation [9], adsorption [10], electrocoagulation [11], ion-exchange and membrane separation [12,13]. Among them, adsorption has been regarded as one of the great potential methods [14].

Chitosan (CS) is a linear cationic semi-synthetic polysaccharide, which could be easily separated from seafood

* Corresponding author.

processing wastes and obtained from the available chitin [15–17]. Because of a large number of amino (pK_a = 6.5) and hydroxyl groups acting as protonated electrostatic and reduction characters, CS has been widely used as a good adsorbent for heavy metals including chromium [18–22]. In consideration of nontoxicity, hydrophilicity, biocompatibility, antibacterial activity and biodegradability, CS was found to be superior to other adsorbents [23,24]. Indeed, numerous studies confirmed CS had adsorption efficiency in Cr(VI) removal, nevertheless, the adsorption capacity was not big as expected [17,20], and could be affected strictly by pH values limited in the range 2.0–4.0. These disadvantages were suggested due to CS characteristics including insufficient functional groups and its pH-dependant charge density [25,26]. Finding ways to overcome these disadvantages is currently one of the major tasks for Cr(VI) adsorption.

Although polymer blends have been tried to modify CS for Cr(VI) adsorption, due to their limited effects on the chemical and physical properties of CS, these disadvantages of CS for Cr(VI) adsorption were little moderated [27,28]. Glutaraldehyde (GA) as a cross-linker was served to modify surface natures of CS containing polymer blends via the carbodiimide activation, which could enhance the exposure of its functional groups and the insensitivity to solution pH, and then accelerate the adsorption rate for Cr(VI) adsorption [29,30].

Poly(vinyl alcohol) (PVA) riches in hydroxyl functional groups, which has great potential to adsorb and reduce Cr(VI) [31,32]. The cross-link between its hydroxyl groups and aldehyde groups of GA formed the ether and acetal linkages, and leaded the three dimensional network structure which was favorable to pore diffusion of Cr(VI) [33].

Polyacrylamide (PAM) is abundant in amide groups, having a tendency to be protonated and then interact with Cr(VI) anions. The amide group cross-linked with aldehyde group of GA could form the –C=N bond which is easy to be protonated even in neutral medium [34]. This can diminish the effect of the solution pH on its Cr(VI) adsorption capacity. Meanwhile, PAM is a polyelectrolyte with negative charges and supposed to react with the substance (i.e., CS and PVA) with positive charges, and a stable polymeric matrix is then generated. A number of studies have prepared polyacrylamide-chitosan (PAM-CS) complex gel beads and checked its great potential as an adsorbent for the metal ions (including Cu^{2+}, Pb^{2+} and Hg^{2+}) removal [35]. Unfortunately, few studies have conducted on this copolymer as an adsorbent to remove Cr(VI).

The ferric ion (Fe(III)) was introduced to polymer matrix by coordination and resulted in destroying the intramolecular and intermolecular hydrogen bonds. This benefitted exposing functional groups and increasing ion-exchange, and then enhanced adsorption properties for Cr(VI) [36–38].

Given all the points, in present study, the copolymers chitosan/polyacrylamide/poly(vinyl alcohol)/Fe/glutaraldehyde (CPPFG) with corresponding amounts of GA were prepared, and employed to do batch experiments to study Cr(VI) adsorption process, and were characterized via scanning electron microscopy (SEM), Fourier transform infrared spectroscopy (FTIR) and X-ray photoelectron spectroscopy (XPS) to explore their Cr(VI) adsorption mechanism.

2. Materials and methods

2.1. Materials

CS (75%–85% deacetylated chitin, M_n = 50–190 kDa) was purchased from Sigma-Aldrich (St. Louis, USA). PAM (M_w = 1.0 × 10^7 g mol^{-1}), PVA (M_w = 10,000–26,000 g mol^{-1}, degree of hydrolysis was 86%–89%), GA (50% GA in water), and analytical grade $K_2Cr_2O_7$, NaCl, $NaNO_3$, Na_2CO_3, $FeCl_3.6H_2O$, H_2SO_4, H_3PO_4, HCl and NaOH, were all purchased from Merck (Merck KGaA, Darmstadt, Germany). Distilled water was used for preparation of all the solutions in the present study.

2.2. Preparation of CPPFG copolymers

In a 250 mL flask, 1.00 g CS was dissolved in 50 mL acetic acid (2%, v/v). In another flask, PVA (0.25 g) was dissolved in 25 mL distilled water at 70°C, and then PAM solution (0.65 g, 65 mL distilled water) was added and mixed by sonicating for 6 h, and then were dropped into CS solution. The mixed solution was upon overnight immersing to form polymer hydrogel. The hydrogel was then shifted and soaked in distilled water at room temperature for 24 h to be gotten purified. A certain amount of GA (50% GA in water diluted to 10 mL) was added into the purified hydrogel and sonicated for 2.5 h, and then was immersed in ferric chloride solution for another 12 h, finally, the objective copolymer was produced. The copolymer was washed with acetic acid (three times) and distilled water (three times) to remove the unreacted substances, respectively, and then dried in the oven at 60°C for 48 h. The expected copolymer was obtained and kept in a desiccator for use.

The reactions scheme of the CPPFG copolymers preparation is shown in Fig. 1, and the relative amounts of the components are listed in Table 1.

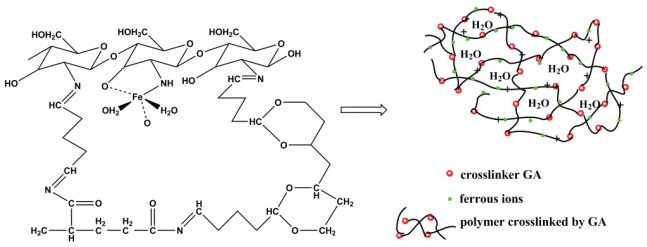

Fig. 1. The chemical reactions preparing the CPPFG copolymers.

Table 1
Relative amounts of the components for the copolymers preparation

Sample name	CS (g)	PAM (g)	PVA (g)	Fe(III) (mol L^{-1})	GA (%)
CPPFG I	1.0	0.65	0.25	0.067	0.26
CPPFG II	1.0	0.65	0.25	0.067	0.76
CPPFG III	1.0	0.65	0.25	0.067	1.20
CPPFG IV	1.0	0.65	0.25	0.067	2.50

2.3. Preparation of Cr(VI) stock and work solutions

The stock solution of Cr(VI) with a concentration of 100.0 mg L^{-1} was obtained by dissolving 0.2829 g of $K_2Cr_2O_7$ in 1,000 mL distilled water, and the designed Cr(VI) concentration solutions were obtained by diluting the stock solution.

2.4. Adsorption experiments

The adsorption experiments were performed via a batch method in a water bath oscillator (500 rpm). CPPFG copolymers (0.1 g) were equilibrated with 50 mL of solution containing various amounts of Cr(VI). The pH was adjusted using 0.1 M solutions of NaOH or HCl.

The amounts of Cr(VI) adsorbed by per unit mass of adsorbent were calculated by Eq. (1):

$$q = \frac{\left(C_0 - C_e\right) \times V}{m} \quad (1)$$

The adsorption removal percentage was evaluated using the following equation:

$$\% \text{ Removal} = \frac{\left(C_0 - C_e\right)}{C_0} \times 100 \quad (2)$$

Here, C_0 and C_e are the initial and equilibrium Cr(VI) concentrations (mg L^{-1}), respectively, q is the Cr(VI) adsorption capacity of the adsorbent (mg g^{-1}), m is the adsorbent mass (g) and V is the solution volume (L).

2.4.1. Effect of pH

To study the influence of initial pH on the removal of Cr(VI), the initial pH values of the solutions were adjusted to 2.5, 4.0, 6.0, 7.0 and 8.0. The CPPFG I, II, III or IV copolymer dose was 2.0 g L^{-1}, Cr(VI) initial concentration (C_0) was 5.0 mg L^{-1} and the temperature (T) was 298 ± 1 K.

2.4.2. Effect of contact time

Kinetic tests were studied for different time intervals (2, 5, 10, 15, 30, 45, 60, 75, 90, 105, 115, 130, 150 and 200 min) at 298 ± 1 K. In each test, 0.1 g CPPFG I, II, III or IV was added to (C_0 = 5.0 or 10.0 mg L^{-1}) 50 mL Cr(VI) solution with pH 6.5.

2.4.3. Effect of initial concentration

Isotherm tests were conducted with different initial Cr(VI) concentrations (C_0 = 5.0, 10.0, 20.0, 25.0, 30.0, 35.0 and 50.0 mg L^{-1}) at an equilibrium time of 4 h in the test condition (adsorbent dose = 2.0 g L^{-1}, pH = 6.5, T = 298 ± 1 K).

2.4.4. Effect of temperature

The conditions for the tests were same as that for the effect of contact time but the temperatures 288 ± 1 K, 298 ± 1 K and 313 ± 1 K.

2.5. Desorption and regeneration studies

After Cr(VI) adsorption on CPPFG II, CPPFG II was collected and rinsed with distilled water to remove unabsorbed Cr(VI), and then placed into NaOH solution (0.05, 0.10 or 0.50 mol L^{-1}) and sonicated for 24 h at 298 ± 1 K. After desorption and separation, the adsorbents were still rinsed with distilled water. The above operations were repeated until Cr(VI) concentration was less than its detected limit in washing liquid, the adsorbent was then rinsed with 0.10 mol L^{-1} HCl (twice) and distilled water (three times) in order, finally separated and dried. After completing the above treatments, the adsorbents were regenerated. The adsorption and desorption processes were repeated for three times.

2.6. Methods

FTIR spectra were characterized using a double beam spectrophotometer (Bruker, model Tensor). UV–vis absorbance spectra were obtained by ultraviolet–visible spectrophotometer (UV-vis Lambda 35). Residual Cr(VI) concentrations are determined by UV–vis spectrophotometer using 1,5-diphenylcarbazide after separation [39]. XPS analysis was made on an ESCALAB 250 Xi spectrometer (Thermo, America) with an Al Kα X-ray source, operated at 10 mA and 15 kV. The surface morphologies of the adsorbents were studied using SEM of a TESCAN VEGA 3 microscope with an accelerating voltage of 10 kV. The pH of the zero point charge (pH_{zpc}) was estimated by zeta potential measurements.

3. Results and discussion

3.1. Characterization

3.1.1. FTIR analysis

The FTIR spectra of the raw materials including CS, PAM and PVA have been reported in references [40–44]. The present FTIR spectra (Fig. 2) corresponded with theirs. So, the spectra characteristics were described briefly here. For CS, the peaks at 1,643 and 1,325 cm^{-1} for acetyl amino group, 3,700–3,000 cm^{-1} for –OH stretching or –NH stretching, 1,200–800 and 1,081 cm^{-1} for C–O and C–O–C stretching, 1,580 and 1,315 cm^{-1} for C–N and N–H stretching, were observed. For PAM, the peaks at 3,700–3,000 cm^{-1} for –NH stretching, 2,930 and 2,879 cm^{-1} for the asymmetric and symmetric stretching vibrations of C–H bond of methylene (-CH_2) group, 1,580 and 1,315 cm^{-1} for the overlapping of C–N and N–H stretching, were found. The peaks of PVA at 3,700–3,000 cm^{-1} for the –OH stretching, 2,930 and 2,879 cm^{-1} for the C–H stretching and 1,200–800 cm^{-1} for C–O stretching appeared.

The FTIR spectra of the copolymers (d, e, f, g,) were also presented in Fig. 2(B). Compared with the FTIR spectra of their raw materials, it was found that the δ (–NH_2) band at 1,596 cm^{-1} was disappeared, the imine band ν_{as}(C=N) at 1,675–1,680 cm^{-1} was formed and ether band (C–O–C) at 1,071 cm^{-1} was enhanced. The intensity of the peak at around 1,670 cm^{-1} relative to ν_{as}(C=N) depends on the level of GA cross-linked [45,46]. The OH and NH stretching bands were narrower and weaken in copolymers, resulted from the destroyed hydrogen bonding between –OH and –NH_2 groups. The intensity at 1,075 cm^{-1} (HO–C) got lower, indicating the HO–C moiety coordinated with Fe^{3+} [47]. All these show the new copolymers were prepared in the present study.

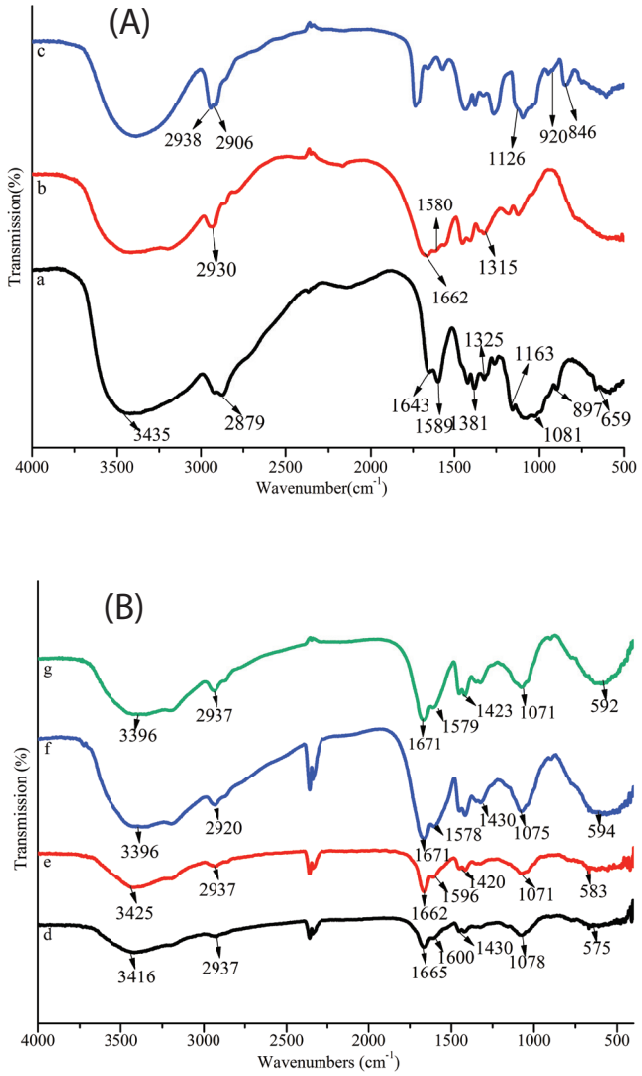

Fig. 2. FTIR spectra of CS (a), PAM (b), PVA (c), CPPFG I (d), CPPFG II (e), CPPFG III (f) and CPPFG IV (g).

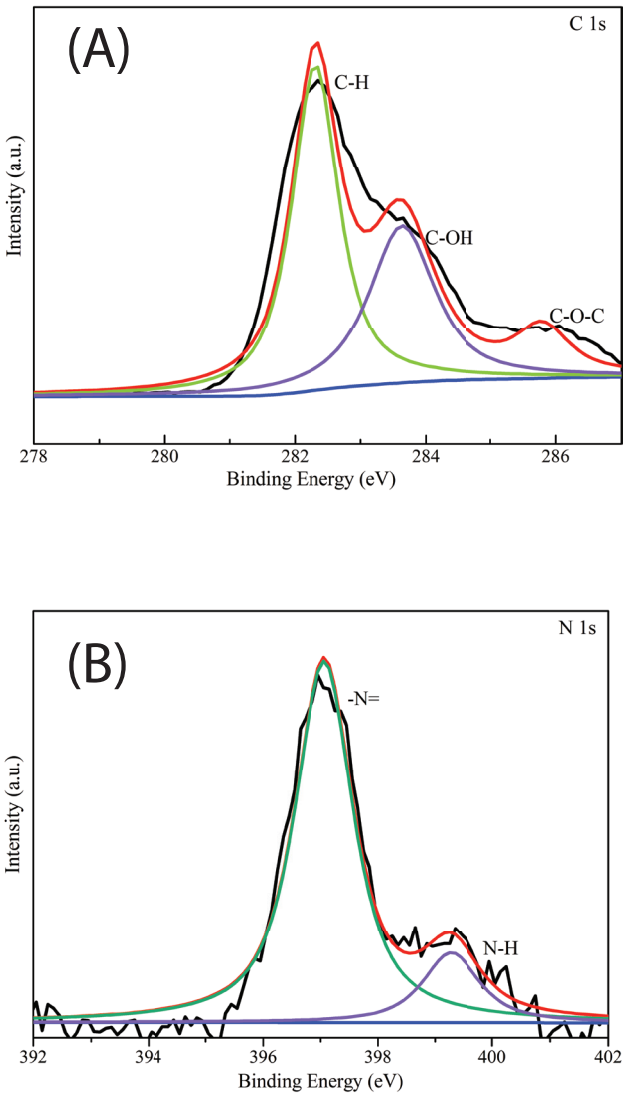

Fig. 3. XPS spectra of CPPFG IV before Cr(VI) adsorption ((A), (B) and (C) are the C, N and O spectra, respectively).

3.1.2. XPS analysis

Fig. 3 shows the XPS scan spectra of the copolymer CPPFG IV. In Fig. 3, three components at 282.37, 283.70 and 285.81 eV in the C 1s region are observed, consistent with C–H, C–OH and C–O–C, respectively. N 1s peak was fitted into two peaks of –N= (binding energy of 397.08 eV) and –NH– (binding energy of 399.25 eV), while O 1s was assigned to one peak (binding energy of 529.84 eV). All these agreed with the results of FTIR analysis.

3.1.3. SEM analysis

SEM images of CPPFG I, II, III and IV before the adsorption ((A), (B), (C) and (D), respectively) and CPPFG III after the adsorption (E) are shown in Fig. 4. It shows that the copolymers possess irregular porous structure with high extent of porosity. In particular, the network morphology with irregular distribution of pores and, the obvious variation of morphology were also found in the copolymers. In the cases of

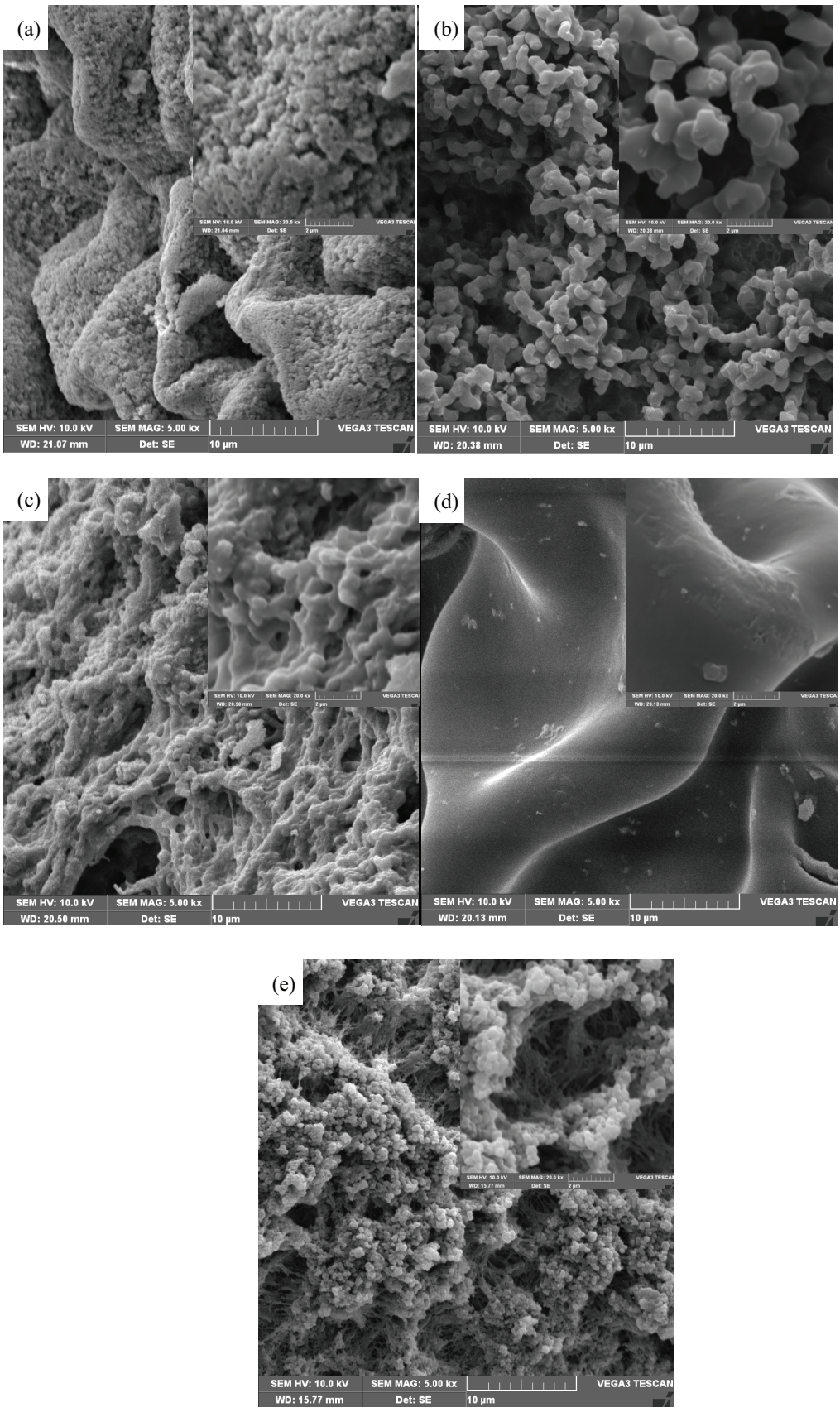

Fig. 4. SEM images of the copolymers before ((a)–(d) for CPPFGs I–IV, respectively) and after adsorption on CPPFG III (e).

CPPFG I and IV, the copolymers with much lower or higher cross-linking density had smaller pore size. An opposite effect can be seen for CPPFG II and III where the pore size appeared larger. Copolymers with greater cross-link density (physical and chemical cross-link) were formed and seemed to be more flat and dense when sufficient water was removed from the pores in the product since the gel network collapses [27,48,49]. As a result, proper amount of GA is beneficial to the better pore structure formation. Also, it can be found that the CPPFG III after Cr(VI) adsorption seems to form small aggregates in the surface of the adsorbent.

3.2. pH_{zpc} of the adsorbents and effect of pH on Cr(VI) adsorption

The zeta potentials of the copolymers and their raw materials at different pH values were determined and are shown in Fig. 5. The effects of initial pH (from 2.0 to 8.0) on Cr(VI) removal by CPPFG I, II, III and IV were studied, respectively, and their results are shown in Fig. 6.

Fig. 5 shows that the pH_{zpc} for CS is 9.1, for CPPFG I approximately is 7.2. It is well known, when the solution pH is less than the adsorbent's pH_{zpc}, the adsorbent's surface is protonated and resulted in having a positive charge [48], so the adsorbent has much great potential to attract anions (such as Cr(VI) anion) via electrostatic interaction. This implies CPPFG as adsorbent can be used in a wider pH range than CS.

From Fig. 6, removal for all the copolymers increased gradually with pH increasing from 2.5 to 4.0, and kept nearly stable within a wide pH range from 4.0 to 7.0; with increasing continuously from 7.0 to 8.0, removal just decreased slightly still at almost 99.0%. All these show that, the copolymers for Cr(VI) adsorption were insensitive to pH variation, and the optimal pH was a wide range from 4.0 to 7.0. Differently, the optimal pH for the collected reported adsorbents usually was a special pH value (Table 2), not a range. This special characteristic of the prepared copolymers might is due to their pH_{zpc}.

In the present study, the solution pH may exert effect on Cr(VI) adsorption in two ways. The surface charges of the adsorbents and the speciation of Cr(VI) are affected by the solution pH. When the pH is less than pH_{zpc} of the adsorbent, the adsorbent surface will be protonated and is positive. To the present study, the protonation worked by hydrogen ions presented in the imine and hydroxyl groups of the adsorbents in acid even neutral solutions [45]. So, these made the adsorbent surface potential electropositive, which is benefit to Cr(VI) adsorption. Cr(VI) can be existed in several species,

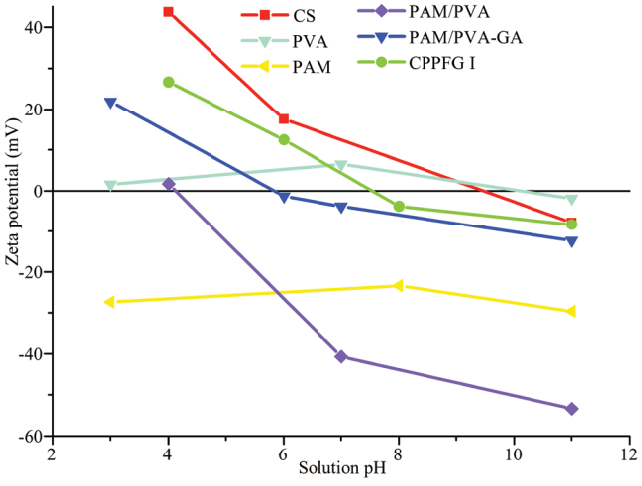

Fig. 5. Zeta potentials of CS, PVA, PAM, PVA/PAM, PVA/PAM-GA and CPPFG I in the solutions with different pH values.

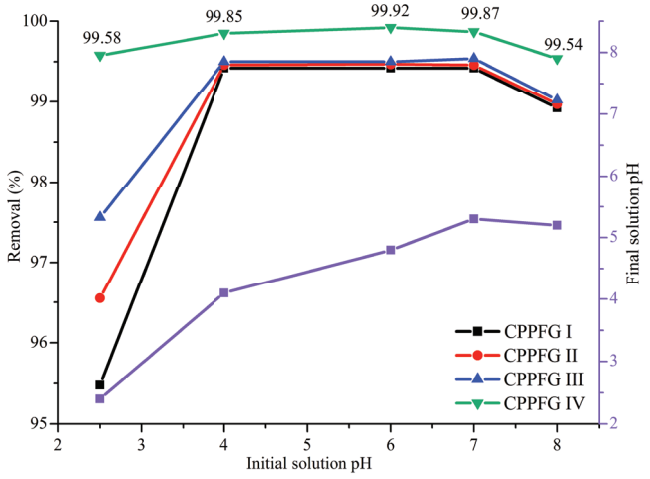

Fig. 6. Effect of initial solution pH on Cr(VI) adsorption removal (C_0 = 5.0 mg L^{-1}, dose = 2.0 g L^{-1}, 298 ± 1 K).

Table 2
The adsorption capacities and optimal pHs of CPPFG IV copolymer and other adsorbents

Adsorbent	Adsorption capacity (mg g^{-1})	C_0 (Cr(VI)) (mg L^{-1})	Optimal pH	Equilibrium time (min)	Reference
Chitosan	22.1	15.0–95.0	3.0	180	[5]
Cross-linked chitosan	11.0	6.0	3.0	600	[51]
Biofunctional magnetic beads	5.8	5.0–40.0	1.0	720	[52]
Hydrolyzed Polyacrylamide-chitosan	13.3	200.0–1,000.0	4.2	400	[53]
Magnetic chitosan beads	106.5	200.0	5.0	600	[54]
Poly(ethylene-*co*-alcohol) nanofiber	11.2	50.0	2.0	60	[55]
Fe_3O_4 NPs/CS/glyoxal/PVA	33.0	5.0–30.0	3.0	90	[33]
CPPFG IV	27.0	5.0–50.0	2.5–7.0	20 or 60	Present work

such as H_2CrO_4, $Cr_2O_7^{2-}$, $HCrO_4^-$ and CrO_4^{2-}. Whose relative concentrations heavily depend on the solution pH. The predominant Cr(VI) specie is $HCrO_4^-$ at pH < 6.51, while CrO_4^{2-} at pH > 6.51 [22,50]. The reported adsorbents prefer to adsorb $HCrO_4^-$ rather than CrO_4^{2-}, because their optimal pH < 6.51 (Table 2). Unlike these, the copolymers have a wide optimal pH range from 4.0 to 7.0, and adsorb both of the species without selectivity.

3.3. Adsorption isotherm

Fig. 7 shows the Cr(VI) adsorption isotherms. From Fig. 7, it can be seen that the copolymers as adsorbents were effective to adsorb Cr(VI), and the effectiveness was hardly affected by the Cr(VI) initial concentration variation from 5.0 to 50.0 mg L^{-1}. The Cr(VI) equilibrium concentrations were lower than its detected limit 0.005 mg L^{-1} in a wide range of initial concentrations within 120 min contact time.

Adsorption capacity was evaluated by determining Cr(VI) equilibrium concentration. Langmuir, Freundlich, Temkin and Dubinin–Radushkevich (D-R) models [56–58] were used to analyze the adsorption isotherm in the present study. The models are expressed as follows:

$$\text{Langmuir: } q_e = \frac{q_m K_L C_e}{1 + K_L C_e} \tag{3}$$

$$R_L = \frac{1}{1 + K_L C_0} \tag{4}$$

$$\frac{C_e}{q_e} = \frac{C_e}{Q_{\max}} + \frac{1}{K_L Q_{\max}} \tag{5}$$

$$\log\left(q_e - q_t\right) = \ln q_e - \frac{K_1}{2.303} t \tag{6}$$

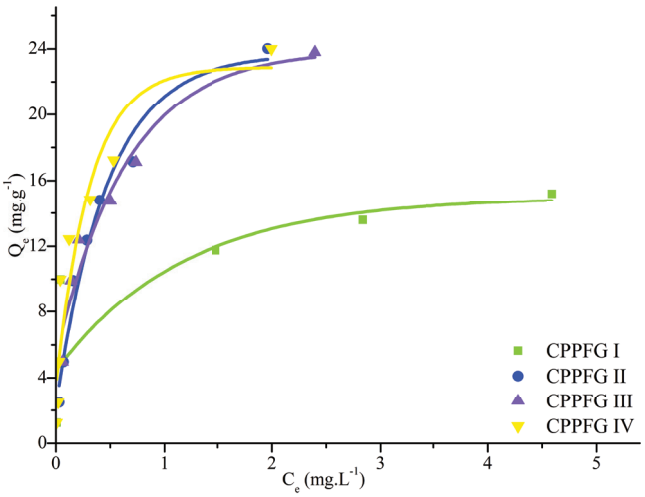

Fig. 7. The relation between equilibrium concentrations and equilibrium adsorption amounts (dose = 2.0 g L^{-1}, pH = 6.5, T = 298 ± 1 K).

$$\text{Freundlich: } q_e = K_F C_e^{1/n} \tag{7}$$

$$\log q_e = \log K_F + \frac{1}{n} \log C_e \tag{8}$$

$$\text{Temkin: } q_e = B_t \ln K_t + B_t \ln C_e \tag{9}$$

$$\text{D-R: } \ln q_e = \ln X_m - K_{\text{DR}} \varepsilon^2 \tag{10}$$

$$\varepsilon = RT \ln\left(1 + \frac{1}{C_e}\right) \tag{11}$$

$$E = -\left(2K_{\text{DR}}\right)^{-0.5} \tag{12}$$

where C_e is the equilibrium concentration (mg L^{-1}), C_0 is the initial concentration (mg L^{-1}), q_e is the amount of Cr(VI) adsorbed at equilibrium (mg g^{-1}) and q_m is the maximum adsorption capacity (mg g^{-1}). R_L is the Langmuir separation factor, K_L is the Langmuir constant related to the affinity of the binding sites (L mg^{-1}), K_F and n are the Freundlich constants connected with the adsorption capacity and intensity. B_t is related to the heat of adsorption and K_t is the equilibrium binding constant. X_m is the adsorption capacity (mg g^{-1}) and K_{DR} is the constant related to adsorption energy (mol² kJ^{-2}). T is the temperature (K), R is the gas constant (8.314 J mol^{-1} K^{-1}) and E (kJ mol^{-1}) is the mean free energy of adsorption.

Langmuir, Freundlich, Temkin and D-R isotherms parameters for Cr(VI) adsorption on CPPFG I, II, III and IV were determined and are listed in Table 3. Table 3 shows that R^2 for Langmuir isotherm was the biggest, indicating that the adsorption process followed Langmuir isotherm model. R_L is the Langmuir separation factor, in all the tests, its values were in the range of 0–1, indicating that the Cr(VI) adsorption on CPPFG I, II, III and IV was favorable.

3.4. Thermodynamic analysis

Thermodynamic parameters such as Gibbs free energy (ΔG^0), enthalpy (ΔH^0) and entropy (ΔS^0) were calculated by the following equations and used to do thermodynamic analysis of the adsorption process onto CPPFG IV:

$$K_d = \frac{\left(C_0 - C_e\right)V}{mC_e} \tag{13}$$

$$\Delta G^0 = -RT \ln K_d \tag{14}$$

$$\ln K_d = \frac{-\Delta H^0}{RT} + \frac{\Delta S^0}{R} \tag{15}$$

where K_d, T and R are the adsorption equilibrium constant, the absolute temperature (K) and the gas constant (J mol^{-1} K^{-1}), respectively.

Table 3
Adsorption equilibrium constants obtained from Langmuir, Freundlich, Temkin and D-R isotherms for Cr(VI) adsorption onto CPPFG I, II, III and IV at 298 ± 1 K

Isotherms	Parameters	CPPFG I	CPPFG II	CPPFG III	CPPFG IV
Langmuir	Q_{max} (mg g^{-1})	14.959	27.647	26.309	25.465
	K_L (L mg^{-1})	8.409	2.999	3.403	6.448
	R^2	0.9901	0.9930	0.9902	0.9903
	R_L (C_0 = 5.0 mg L^{-1})	0.023	0.063	0.056	0.030
Freundlich	K_F (L mg^{-1})	11.017	21.147	18.971	24.874
	n	3.323	1.853	2.547	1.989
	R^2	0.7001	0.9292	0.8927	0.8101
Temkin	B_t	1.893	5.178	4.882	4.097
	K_t (L mg^{-1})	573.524	43.527	49.289	149.291
	R^2	0.8624	0.9863	0.9834	0.9589
D-R	K_{DR} (mol^2 kJ^{-2})	0.015	0.029	0.029	0.020
	X_m (mg g^{-1})	15.216	20.269	20.863	22.278
	R^2	0.8991	0.9768	0.9583	0.9394
	E (kJ mol^{-1})	5.774	4.152	4.1812	5.051
	q_{exp} (mg g^{-1})	15.206	26.819	25.230	24.002

Table 4
The isotherm model constants and correlation coefficients for the adsorption of Cr(VI) by CPPFG IV at 288, 298 and 323 ± 1 K

Isotherms	Parameters	288 K	298 K	323 K
Langmuir	Q_{max} (mg g^{-1})	23.546	25.465	26.302
	K_L (L mg^{-1})	3.162	6.448	15.455
	R^2	0.9849	0.9902	0.9968
Freundlich	K_F (L mg^{-1})	14.659	24.873	41.355
	n	2.809	1.989	1.886
	R^2	0.7551	0.8101	0.8451
Temkin	B_t	2.454	4.097	4.433
	K_t (L mg^{-1})	328.389	149.291	300.155
	R^2	0.5782	0.9589	0.9605
D-R	K_{DR} (mol^2 kJ^{-2})	0.017	0.019	0.012
	X_m (mg g^{-1})	16.434	22.278	26.341
	R^2	0.3539	0.9394	0.9819
	E (kJ mol^{-1})	5.423	5.051	6.455
q_{exp} (mg g^{-1})		22.213	24.002	25.268
ΔG^0 (kJ mol^{-1})		–10.576	–11.963	–15.782

The thermodynamic parameters for Cr(VI) adsorption onto CPPFG IV were determined and are listed in Table 4.

Table 4 shows that ΔG^0 for all the study temperatures are negative, and get smaller with temperature rising (–10.576 kJ mol^{-1} at 288 K, –11.963 kJ mol^{-1} at 298 K and –15.782 kJ mol^{-1} at 323 K). This negative ΔG^0 indicates that the adsorption process was spontaneous in nature. Increasing magnitude of ΔG^0 shows that rising temperature increases the degree of reaction spontaneity [59].

ΔH^0 and ΔS^0 were calculated from the slope and intercept of $\ln K_d$ vs. $1/T$ and 32.50 kJ mol^{-1} and 149.03 J mol^{-1} K^{-1}, respectively. ΔH^0 value (32.50 kJ mol^{-1}) confirms that the Cr(VI) adsorption is an endothermic process, which is consistent with the results of the adsorption isotherm. The positive value of ΔS^0 (149.03 J mol^{-1} K^{-1}) suggests the increased randomness at the adsorbent/solution interface for Cr(VI) adsorption on the copolymers.

3.5. Kinetic studies

The Cr(VI) adsorption behaviors onto CPPFG I, II, III and IV are shown in Fig. 8. It shows that the adsorption was very fast and dramatically increased at the beginning, and then reached equilibrium. Especially, the adsorption on CPPFG III and IV could attain equilibrium within 20 min. The other copolymers attained their adsorption equilibrium within 60 min. Compared with the reported adsorbents for Cr(VI) adsorption (Table 2), the present studied copolymers were very efficient in reaching the adsorption equilibrium. This might be due to the existence of GA in the copolymers, which could form more carbodiimide binds among polymer matrix and enhance electrostatic interaction and thus accelerate the adsorption rate [10,18]. The results are in agreement with the intraparticle diffusion analysis discussed as follows.

To further investigate the Cr(VI) adsorption behavior on the studied copolymers, the pseudo-first-order kinetics [33], the pseudo-second-order kinetics [4] and intraparticle diffusion models [12] were fitted. The pseudo-first-order equation is as follows:

$$\frac{1}{q_t} = \frac{K_1}{q_e t} + \frac{1}{q_e} \tag{16}$$

where q_e and q_t (mg g^{-1}) are the adsorption quantities at equilibrium and unequilibrium time (min), respectively; K_1 is the rate constant (min^{-1}) and t is adsorption time.

The pseudo-second-order kinetic model is expressed by the following equation:

$$\frac{t}{q_t} = \frac{1}{K_2 q_e^{\,2}} + \frac{t}{q_e} \tag{17}$$

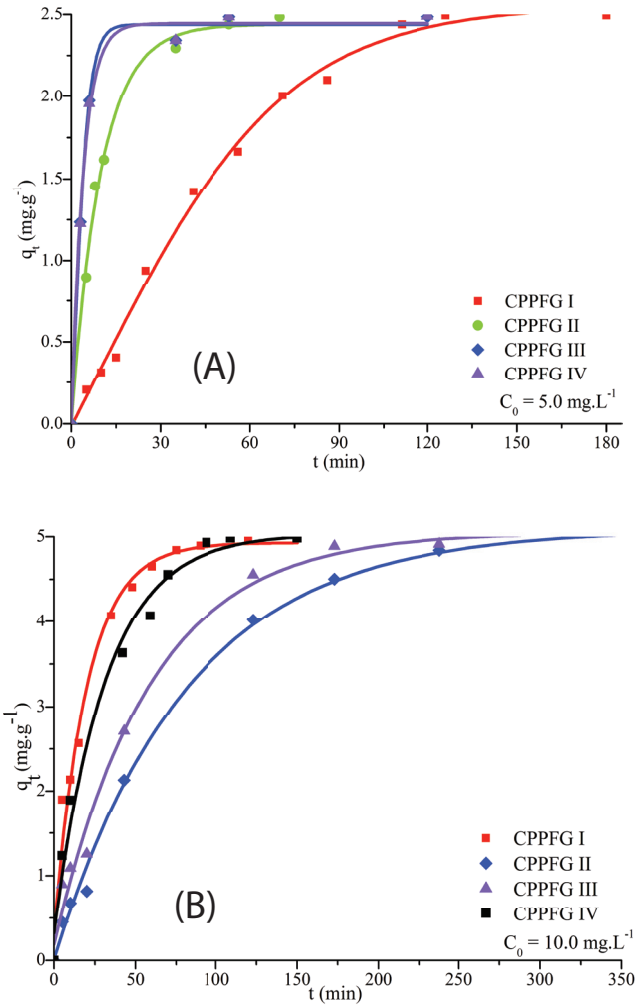

Fig. 8. Effect of contact time on Cr(VI) adsorption onto CPPFG I, II, III and IV copolymers. (A) C_0 = 5.0 mg L^{-1} and (B) C_0 = 10.0 mg L^{-1} (dose = 2.0 g L^{-1}, pH = 6.5, T = 298 ± 1 K).

where K_2 is the equilibrium rate constant (g mg^{-1} min^{-1}). The slope and intercept of plotting of t/q_t vs. t are used to calculate the constant K_2.

The intraparticle diffusion kinetic equation is as follows:

$$q_t = K_{id} t^{0.5} + C_{id} \quad (18)$$

where K_{id} and C_{id} are the rate constants.

The parameters of the pseudo-second-order and pseudo-second-order models were calculated for the present tests and are listed in Table 5.

Table 5 shows that R^2 for the pseudo-second-order model was much larger than the other, and the calculated q_e agreed well with the experimental data (q_{exp}). So, the kinetic data were better described by the pseudo-second-order model. The result further illustrated the combined effects of chemisorptions and physisorptions in the adsorption process. K_2 of the pseudo-second-order model, got smaller with increasing Cr(VI) concentration from 5.0 to 50.0 mg L^{-1}, implying the advantages of the adsorptions at Cr(VI) low concentration [18,23].

The three linear portions in the plots of q_t vs $t^{0.5}$ (Fig. 9) demonstrated that the adsorption for Cr(VI) by adsorbents via three steps which were external surface adsorption, mesopore and micropore diffusion [30,60]. As shown in Fig. 9(A), the $K_{id,1}$ values in the kinetic adsorption processes on CPPFG II, III and IV were much higher than $K_{id,2}$ and $K_{id,3}$ values, indicating the adsorption process from the bulk phase to the exterior surface of the adsorbents should be the rate-controlling step [61]. The values of $K_{id,3}$ were close to zero, denoting that the micropore diffusion was not apparent in this system. It could be concluded that the external surface adsorption rate determined the overall adsorption rate at low Cr(VI) concentrations. The adsorbents with higher GA cross-link densities could form more cross-linking sites served as electrostatic interactions (–C=N) and attenuated repulsive forces with Cr(VI) anions. While in Fig. 9(B), at 10.0 mg L^{-1} Cr(VI) concentration, the $K_{id,2}$ values are much higher than $K_{id,1}$ and $K_{id,3}$, indicating that the mesopore diffusion ruled in the adsorption process. The adsorbent CPPFG I had the well-connected pores as well as ample available binding sites for Cr(VI) adsorption leading to relatively faster adsorption rate.

3.6. Effect of coexisting anions on Cr(VI) adsorption

Chloride (Cl^-), nitrate (NO_3^-) and carbonate (CO_3^{2-}) are main anions in aqueous systems. They may compete with the target anion Cr(VI) for active sites on the adsorbent, and are selected as coexisting anions and employed to do the experiments to study their effect on Cr(VI) adsorption. The data are shown in Fig. 10. Three kinds of anions at 5.0 mg L^{-1} initial Cr(VI) concentration were carried out, and the added anion concentrations ranged from 0.01 to 0.05 mol L^{-1}.

Fig. 10 shows that the removal percentage of Cr(VI) decreased as the result of the anion addition. The higher the absolute value of anion valence is, the greater decrease is. In another words, the Cr(VI) adsorption capacity was slightly affected by the presence of anions. This benefits the adsorbents applying in practice, which also implies that the adsorption is via electrostatic interaction.

3.7. Desorption characteristics

The reusability of adsorbent materials is an important factor for a cost-effective water treatment. The desorption experiments were conducted in 0.05, 0.1 or 0.5 mol L^{-1} NaOH solution, respectively. Their results are shown in Fig. 11. It shows that during the adsorption–desorption three cycles, the adsorption capacity remained high to 65% of the initial capacity, and the Cr(VI) equilibrium concentrations were also lower than its detected limit. This showed that NaOH solution as desorption solution was efficient, and its optimal concentration approximately was 0.05 mol L^{-1}. These results are consistent with that of the other reports [33,40,43], and also imply that the copolymers have a potential to be used as adsorbents for Cr(VI) removal.

3.8. Cr(VI) adsorption removal primary mechanism

Fig. 12 shows FTIR spectra of CPPFG IV before and after Cr(VI) adsorption. Compared the FTIR spectra of CPPFG IV before (d) and after Cr(VI) adsorption (k), it was found that

Table 5
The pseudo-first-order model and the pseudo-second-order model parameters for Cr(VI) adsorption on CPPFG I, II, III and IV copolymers

C_0 (mg L^{-1})	q_{exp} (mg g^{-1})	Pseudo-first-order			Pseudo-second-order		
		K_1	q_e	R^2	K_2	q_e	R^2
CPPFG I							
5.0	2.489	20.2521	2.035	0.9842	0.0222	2.114	0.9922
10.0	4.985	19.4630	6.007	0.9785	0.0141	5.514	0.9966
20.0	9.983	35.6612	11.589	0.9821	0.0039	10.634	0.9987
25.0	11.825	159.5103	14.369	0.9484	0.0009	12.303	0.9972
30.0	14.583	771.7901	26.469	0.8881	0.0003	15.711	0.9934
35.0	15.206	252.3703	18.106	0.6711	0.0002	17.529	0.9807
CPPFG II							
5.0	2.485	7.6049	2.746	0.9892	0.0681	2.640	0.9984
10.0	5.993	90.9621	6.687	0.9903	0.0024	6.030	0.9904
20.0	9.922	155.2323	12.694	0.7646	0.0015	10.501	0.9922
25.0	12.398	205.7714	15.843	0.7945	0.0008	13.231	0.9924
30.0	14.799	209.6320	19.463	0.8860	0.0006	16.229	0.9909
35.0	17.109	61.7084	17.797	0.8833	0.0001	17.659	0.9997
50.0	24.013	61.2082	26.212	0.9558	0.0001	24.667	0.9994
CPPFG III							
5.0	2.499	1.6510	2.513	0.9658	0.2179	2.527	0.9996
10.0	4.965	53.0542	6.131	0.9686	0.0055	5.533	0.9917
20.0	9.952	37.1491	10.251	0.7967	0.0035	10.102	0.9996
25.0	12.411	60.8403	12.767	0.8864	0.0014	12.647	0.9981
30.0	14.664	192.7304	18.727	0.8910	0.0005	16.147	0.9951
35.0	17.053	71.3657	17.797	0.8934	0.0006	18.057	0.9996
50.0	23.980	28.0081	24.944	0.9763	0.0001	24.963	0.9993
CPPFG IV							
5.0	2.486	1.7371	2.518	0.9701	0.2060	2.533	0.9996
10.0	4.985	30.2070	6.293	0.9337	0.0072	5.915	0.9872
20.0	9.980	53.1834	11.623	0.9202	0.0022	10.923	0.9962
25.0	12.879	46.5011	14.081	0.9928	0.0019	13.656	0.9982
30.0	14.843	55.5690	15.954	0.9661	0.0017	15.342	0.9994
35.0	17.165	49.1096	18.460	0.9857	0.0017	17.753	0.9993
50.0	24.002	202.8322	26.624	0.9899	0.0002	26.911	0.9981

several peaks had changed from 2,937 to 2,940 cm^{-1} (blue-shift), 1,620 to 1,600 cm^{-1} (red-shift), 1,420 to 1,400 cm^{-1} (red-shift), 1,078 to 1,062 cm^{-1} (red-shift) and 594 to 585 cm^{-1} (red-shift) [61]. These revealed that these functional groups including –C=N, –NH, –C–O and –OH were involved in Cr(VI) adsorption.

Fig. 13 shows the XPS scan spectra of CPPFG IV after Cr(VI) adsorption, and (A), (B), (C) and (D) peaks corresponds to C 1s, N 1s, O 1s and Cr 2p, respectively. N 1s peak was deconvoluted into three peaks, –N= at 397.01 eV, N–H at 399.38 eV and $–N=^+$ at 400.02 eV [32]. Compared with Fig. 3, after Cr(VI) adsorption, a new peak at 400.02 eV appeared as a result of the protonated quinoid imine units ($–N=^+$) [8,18,32], and implies the adsorbent with positive charge. This is agreed with the result of the adsorption isotherm models. The E values (Table 3) lying 1 and 8 kJ mol^{-1} showed that the Cr(VI) adsorption was governed via electrostatic interaction [41]. Because of this protonation less depending on solution pH, Cr(VI) adsorption was insensitive to the solution pH variation and kept its high efficiency [62]. Even though, the peak at 397.01 eV for –N= was still presented after the adsorption.

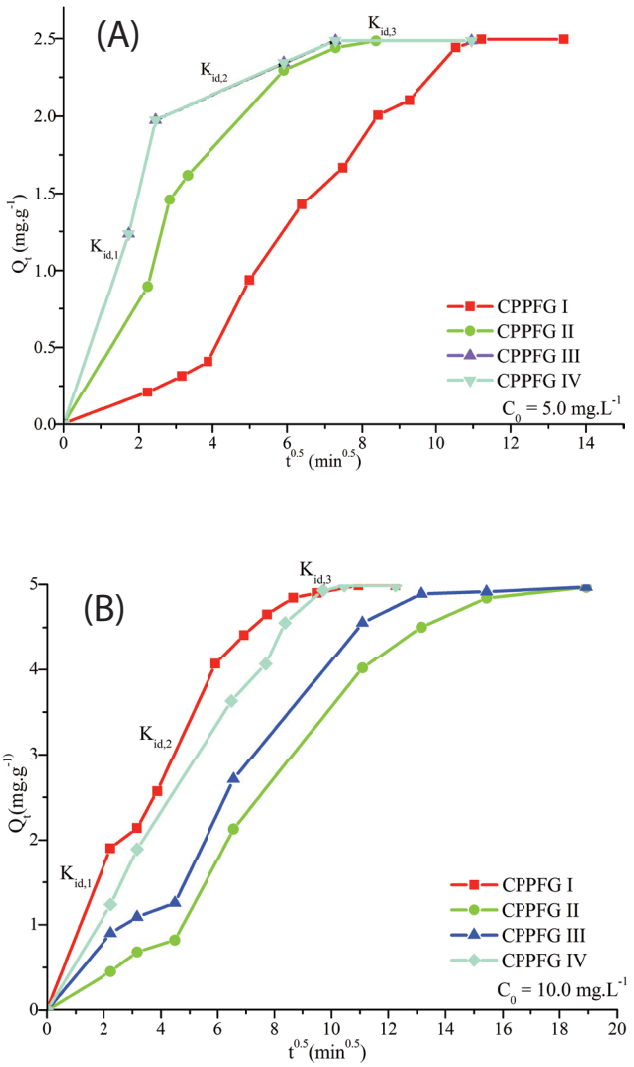

Fig. 9. Kinetic models of intraparticle diffusion at different stages. (A) C_0 = 5.0 mg L^{-1} and (B) C_0 = 10.0 mg L^{-1} (dose = 2.0 g L^{-1}, T = 298 ± 1 K).

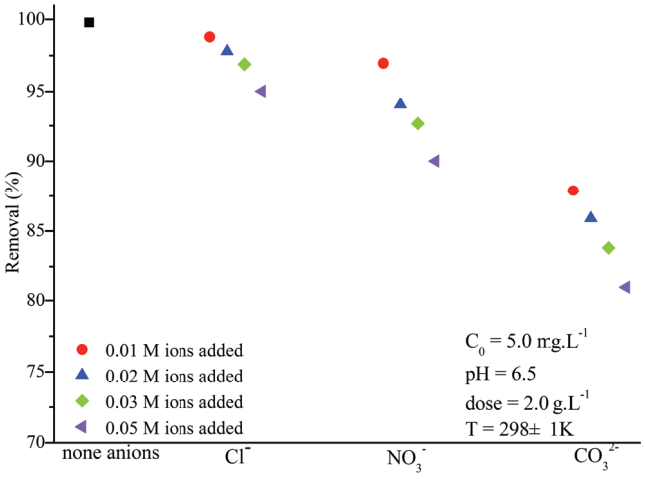

Fig. 10. Effect of anions on Cr(VI) removal (C_0 = 5.0 mg L^{-1}, T = 298 ± 1 K, pH = 6.5, dose = 2.0 g L^{-1}).

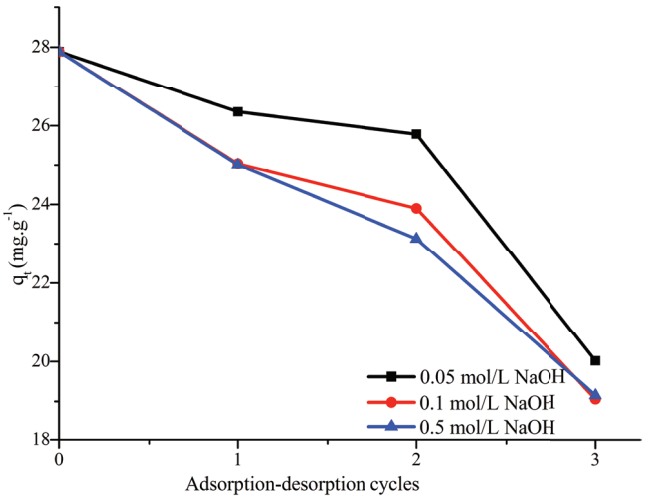

Fig. 11. Adsorption–desorption cycles study for Cr(VI) from aqueous solution by CPPFG II (dose = 2.0 g L^{-1}, T = 298 ± 1 K, C_0 = 50.0 mg L^{-1}, pH = 6.5).

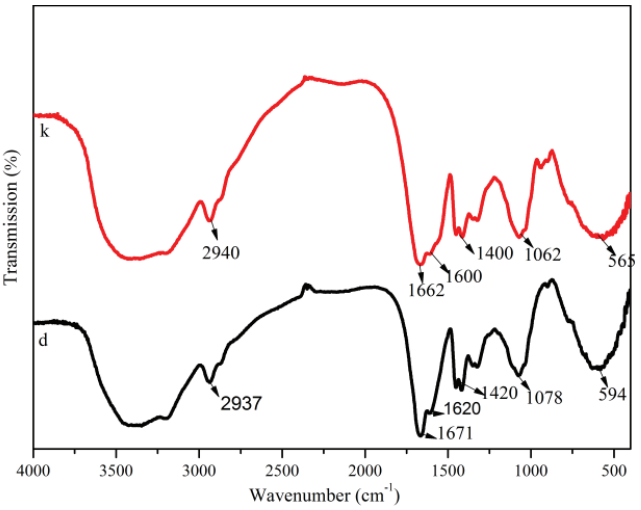

Fig. 12. FTIR spectra of CPPFG IV before and after Cr(VI) adsorption.

This possibly due to the consumption of Cr(VI) as well as proton retarded and eventually terminated the redox reaction to Cr(III) [32]. The two peaks at 569 and 574 eV ascribed to Cr(III) and the peak at 576 eV for Cr(VI) were observed [63].

Based on above, it could be concluded that the Cr(VI) adsorption removal process covered three important types of reactions: (1) electrostatic attraction, (2) reduction and (3) precipitation. Cr(VI) was absorbed first by the protonated groups (such as –OH and –C=N) and then partially reduced to Cr(III). Some of the Cr(III) ions were absorbed via electrostatic attraction with C–O and –N–H on the absorbents surface [64,65]. The other part of the Cr(III) ions precipitated. This is the main reason why the adsorption capacity got slightly decreased in the adsorption–desorption cycling process. The primary mechanism for the Cr(VI) adsorption removal was shown in Fig. 14. During the adsorption process, OH^- could also be adsorbed on the adsorbents and caused H^+ releasing

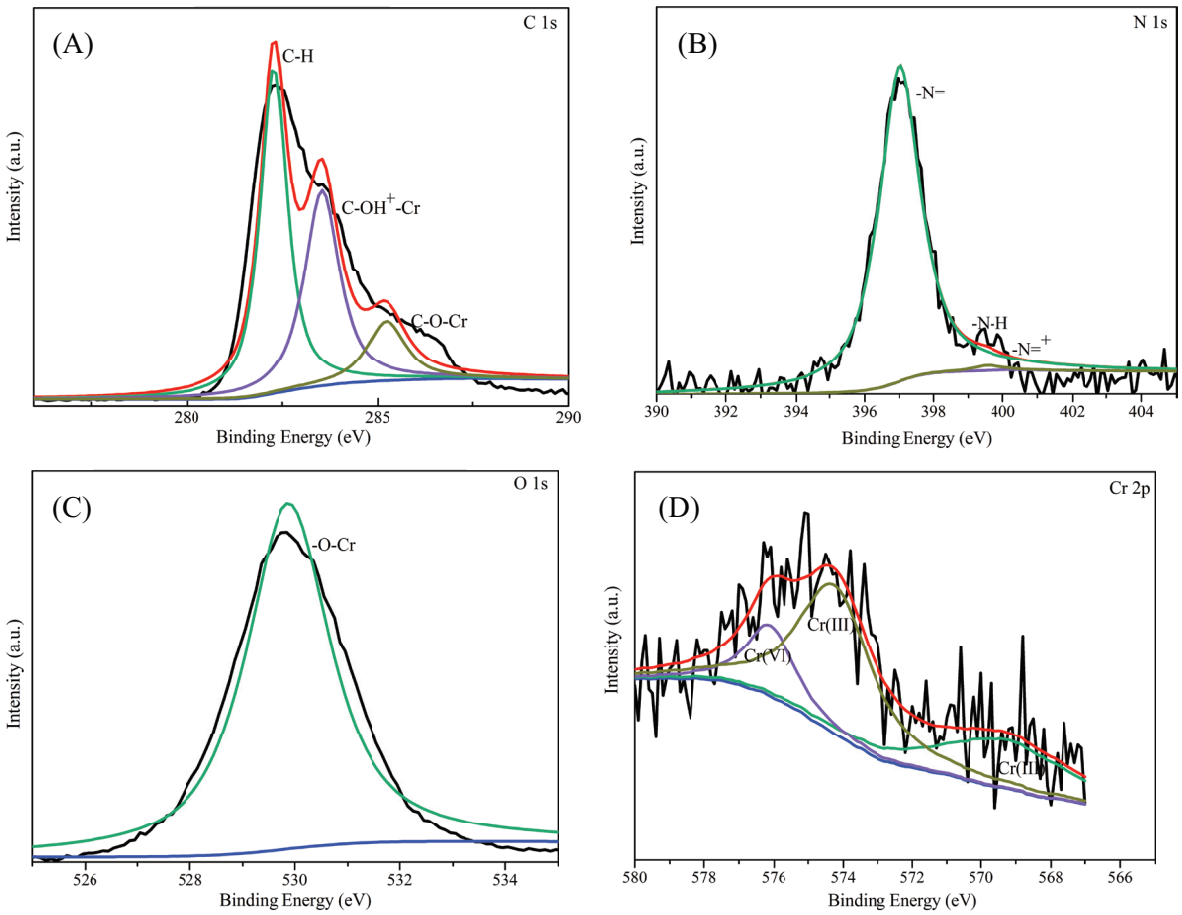

Fig. 13. XPS spectra of CPPFG IV after Cr(VI) adsorption ((A), (B), (C) and (D) were the C, N, O and Cr spectra, respectively).

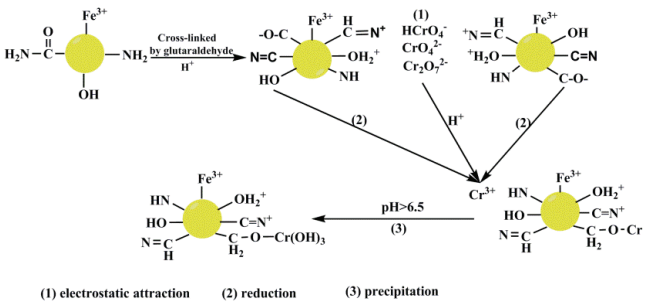

Fig. 14. The primary mechanism of Cr(VI) adsorption removal by the adsorbent.

into the solution and resulted in a slight decrease of the solution pH, which were consistent with the results of XPS and deduction of O–Cr bond formation [66].

4. Conclusions

This study presents the synthesis and characterization of the CPPFG copolymers as new adsorbents, and its adsorption properties and mechanism for Cr(VI) adsorption removal. The results showed that the copolymers had a fast adsorption rate and high adsorption efficiency above 99.50% which was hardly affected by initial pH values varying from 3.0 to 8.0 and the coexisting anions. The adsorption fitted Langmuir and Temkin isotherm models well. The removal of Cr(VI) followed pseudo-second-order and intraparticle diffusion kinetic models, and its rate was mainly controlled by chemical adsorption and intraparticle mass transport. The calculated thermodynamic parameters (ΔG^0, ΔH^0 and ΔS^0) demonstrated that the adsorption was a spontaneous and endothermic process. The adsorption capacity and rate were strongly depended on the quantity of the available functional binding sites (i.e., –OH, –C=N and –NH), and surface morphologies with different GA cross-link densities under the studied conditions. The possible mechanism was proposed based on the data of FTIR, XPS, SEM and zeta potential.

Acknowledgments

The authors gratefully acknowledge the financial support by the National Natural Science Foundation of China (No. 41502240), the Seed Foundation of Innovation and Creation for Graduate Students in Northwestern Polytechnical University (No. Z2017192), the Natural Science Basic Research Plan in Shaanxi Province of China (No. 2017JM4005), the Fundamental Research Funds for the Central Universities (No. 3102017zy056), the Key Laboratory of Groundwater Contamination and Remediation, China Geological Survey (CGS) and Hebei Province (No. KF201610).

References

[1] P. Miretzky, A.F. Cirelli, Cr(VI) and Cr(III) removal from aqueous solution by raw and modified lignocellulosic materials: a review, J. Hazard. Mater., 180 (2010) 1–19.

[2] A. Mohsenibandpi, B. Kakavandi, R.R. Kalantary, A. Azari, A. Keramati, Development of a novel magnetite–chitosan composite for the removal of fluoride from drinking water: adsorption modeling and optimization, RSC Adv., 5 (2015) 73279–73289.

[3] D.A. Backhus, J.N. Ryan, D.M. Groher, J.K. MacFarlane, P.M. Gschwend, Sampling colloids and colloid-associated contaminants in ground water, Ground Water, 31 (1993) 466–479.

[4] C. Shen, H. Chen, S. Wu, Y. Wen, L. Li, Z. Jiang, M. Li, W. Liu, Highly efficient detoxification of Cr(VI) by chitosan–Fe(III) complex: process and mechanism studies, J. Hazard. Mater., 244–245 (2013) 689–697.

[5] N.N. Thinh, P.T.B. Hanh, L.T.T. Ha, L.N. Anh, T.V. Hoang, V.D. Hoang, L.H. Dang, N.V. Khoi, T.D. Lam, Magnetic chitosan nanoparticles for removal of Cr(VI) from aqueous solution, Mater. Sci. Eng., 33 (2013) 1214–1218.

[6] K. Salnikow, A. Zhitkovich, Genetic and epigenetic mechanisms in metal carcinogenesis and cocarcinogenesis: nickel, arsenic, and chromium, Chem. Res. Toxicol., 21 (2008) 28–44.

[7] F. Gao, H. Gu, H. Wang, X. Wang, B. Xiang, Z. Guo, Magnetic amine-functionalized polyacrylic acid-nanomagnetite for hexavalent chromium removal from polluted water, RSC Adv., 5 (2015) 60208–60219.

[8] M.K. Dinker, P.S. Kulkarni, Recent advances in silica-based materials for the removal of hexavalent chromium: a review, J. Chem. Eng. Data, 60 (2015) 2521–2540.

[9] N. Kongsricharoern, C. Polprasert, Chromium removal by a bipolar electro-chemical precipitation process, Water Sci. Technol., 34 (1996) 109–116.

[10] Q. Li, Y. Qian, H. Cui, Q. Zhang, R. Tang, J. Zhai, Preparation of poly(aniline-1,8-diaminonaphthalene) and its application as adsorbent for selective removal of Cr(VI) ions, Chem. Eng. J., 173 (2011) 715–721.

[11] J. Liu, C. Wang., J. Shi, H. Liu, Y. Tong, Aqueous Cr(VI) reduction by electrodeposited zero-valent iron at neutral pH: acceleration by organic matters, J. Hazard. Mater., 163 (2009) 370–375.

[12] X. Huang, Y. Liu, S. Liu, X. Tan, Y. Ding, G. Zeng, Y. Zhou, M. Zhang, S. Wang, B. Zheng, Effective removal of Cr(VI) using β-cyclodextrin–chitosan modified biochars with adsorption/reduction bifuctional roles, RSC Adv., 6 (2016) 94–104.

[13] J.B. Dima, C. Sequeiros, N.E. Zaritzky, Hexavalent chromium removal in contaminated water using reticulated chitosan micro/nanoparticles from seafood processing wastes, Chemosphere, 141 (2015) 100–111.

[14] C. Lei, X. Zhu, B. Zhu, C. Jiang, Y. Le, J. Yu, Superb adsorption capacity of hierarchical calcined Ni/Mg/Al layered double hydroxides for Congo red and Cr(VI) ions, J. Hazard. Mater., 321 (2017) 801–811.

[15] G. Crini, P.M. Badot, Application of chitosan, a natural aminopolysaccharide, for dye removal from aqueous solutions by adsorption processes using batch studies: a review of recent literature, Prog. Polym. Sci., 33 (2008) 399–447.

[16] J.R.R. de Souza, J.P.A. Feitosa, N.M.P.S. Ricardo, M.T.S. Trevisan, H.C.B. de Paula, C.M. Ulrich, R.W. Owen, Spray-drying encapsulation of mangiferin using natural polymers, Food Hydrocolloids, 33 (2013) 10–18.

[17] W. Kaminski, E. Tomczak, K. Jaros, Interactions of metal ions sorbed on chitosan beads, Desalination, 218 (2008) 281–286.

[18] L. Wu, Z. Qin, F. Yu, J. Ma, Graphene oxide cross-linked chitosan nanocomposite adsorbents for the removal of Cr (VI) from aqueous environments, Desal. Wat. Treat., 72 (2017) 300–307.

[19] P.D. Chethan, B. Vishalakshi, Synthesis of ethylenediamine modified chitosan and evaluation for removal of divalent metal ions, Carbohydr. Polym., 97 (2013) 530–536.

[20] B. Krajewska, Diffusion of metal ions through gel chitosan membranes, React. Funct. Polym., 47 (2001) 37–47.

[21] A.J. Varma, S.V. Deshpande, J.F. Kennedy, Metal complexation by chitosan and its derivatives: a review, Carbohydr. Polym., 55 (2004) 77–93.

[22] S.E. Bailey, T.J. Olin, R.M. Bricka, D.D. Adrian, A review of potentially low-cost sorbents for heavy metals, Water Res., 33 (1999) 2469–2479.

[23] M.G. Rajiv, S. Meenakshi, Preparation of amino terminated polyamidoamine functionalized chitosan beads and its Cr(VI) uptake studies, Carbohydr. Polym., 91 (2013) 631–637.

[24] R.A.A. Muzzarelli, J. Boudrant, D. Meyer, N. Manno, M. Demarchis, M.G. Paoletti, Current views on fungal chitin/chitosan, human chitinases, food preservation, glucans, pectins and inulin: a tribute to Henri Braconnot, precursor of the carbohydrate polymers science on the chitin bicentennial, Carbohydr. Polym., 87 (2012) 995–1012.

[25] H.H. Najafabadi, M. Irani, L.R. Rad, A.H. Haratameh, I. Haririan, Correction: Removal of Cu^{2+}, Pb^{2+} and Cr^{6+} from aqueous solutions using a chitosan/graphene oxide composite nanofibrous adsorbent, RSC Adv., 5 (2015) 22390.

[26] C. Jung, J. Heo, J. Han, N. Her, S.J. Lee, J. Oh, J. Ryu, Y. Yoon, Hexavalent chromium removal by various adsorbents: powdered activated carbon, chitosan, and single/multi-walled carbon nanotubes, Sep. Purif. Technol., 106 (2013) 63–71.

[27] Y. Wu, Y. Zhang, J. Qian, X. Xin, S. Hu, S. Zhang, J. Wei, An exploratory study on low-concentration hexavalent chromium adsorption by Fe(III)-cross-linked chitosan beads, R. Soc. Open Sci., 4 (2017) 170905.

[28] V.M. Boddu, K. Abburi, J.L. Talbott, E.D. Smith, Removal of hexavalent chromium from wastewater using a new composite chitosan biosorbent, Environ. Sci. Technol., 37 (2003) 4449–4456.

[29] S. Wu, J. Hu, L. Wei, Y. Du, X. Shi, H. Deng, L. Zhang, Construction of porous chitosan-xylan-TiO_2 hybrid with highly efficient sorption capability on heavy metals, J. Environ. Chem. Eng., 2 (2014) 1568–1577.

[30] F. Zhao, E. Repo, M. Sillanpaa, Y. Meng, D. Yin, W.Z. Tang, Green synthesis of magnetic EDTA- and/or DTPA-cross-linked chitosan adsorbents for highly efficient removal of metals, Ind. Eng. Chem. Res., 54 (2015) 1271–1281.

[31] L.Y. Wang, M.J. Wang, Removal of heavy metal ions by poly(vinyl alcohol) and carboxymethyl cellulose composite hydrogels prepared by a freeze-thaw method, Sustain. Chem. Eng., 4 (2016) 2830–2837.

[32] T. Wang, L. Zhang, C. Li, W. Yang, T. Song, C. Tang, Y. Meng, S. Dai, H. Wang, L. Chai, J. Luo, Synthesis of core-shell magnetic Fe_3O_4@poly(m-phenylenediamine) particles for chromium reduction and adsorption, Environ. Sci. Technol., 49 (2015) 5654–5662.

[33] M. Mirabedini, M.Z. Kassaee, Removal of toxic Cr(VI) from water by a novel magnetic chitosan/glyoxal/PVA hydrogel film, Desal. Wat. Treat., 57 (2016) 14266–14279.

[34] I. Dmitriev, I. Kuryndin, N. Bobrova, M. Smirnov, Swelling behavior and network characterization of hydrogels from linear polyacrylamide crosslinked with glutaraldehyde, Mater. Today Commun., 4 (2015) 93–100.

[35] J. Cao, Y. Tan, Y. Che, H. Xin, Novel complex gel beads composed of hydrolyzed polyacrylamide and chitosan: an effective adsorbent for the removal of heavy metal from aqueous solution, Bioresour. Technol., 101 (2010) 2558–2561.

[36] M.L. Masheane, L.N. Nthunya, S.P. Malinga, E.N. Nxumalo, B.B. Mamba, S.D. Mhlanga, Synthesis of Fe-Ag/f-MWCNT/PES nanostructured-hybrid membranes for removal of Cr(VI) from water, Sep. Purif. Technol., 184 (2017) 79–87.

[37] P.A. Kavakli, C. Kavakli, O. Guven, Preparation and characterization of Fe(III)-loaded iminodiacetic acid modified GMA grafted nonwoven fabric adsorbent for anion adsorption, Radiat. Phys. Chem., 94 (2014) 105–110.

[38] I. Yoshida, M. Nishimura, K. Matsuo, K. Ueno, Studies of the selective adsorption of anion by metal ion loaded ion-exchange resin. V. Adsorption of phosphate ion on ion-exchange resin loaded with zirconium(IV), IRC 50-Zr(IV), Sep. Purif. Technol., 18 (1983) 73–82.

[39] M. Amara, H. Kerdjoudj, A modified anion-exchange membrane applied to purification of effluent containing different anions. Pre-treatment before desalination, Desalination, 206 (2007) 205–209.
[40] N. Yi, Y. Wu, J. Wei, S. Zhang, P. Ji, Adsorption of the low concentration Cr(VI) on magnetic chitosan/PVA hydrogel beads, Fresenius Environ. Bull., 25 (2016) 2174–2182.
[41] L. Li, L. Fan, M. Sun, H. Qiu, X. Li, H. Duan, C. Luo, Adsorbent for chromium removal based on graphene oxide functionalized with magnetic cyclodextrin–chitosan, Colloids Surf., B, 58 (2013) 169–175.
[42] H. Cui, M. Fu, S. Yu, M.K. Wang, Reduction and removal of Cr(VI) from aqueous solutions using modified by products of beer production, J. Hazard. Mater., 186 (2011) 1625–1631.
[43] N.R. Kildeeva, P.A. Perminov, L.V. Vladimirov, V.V. Novikov, S.N. Mikhailov, About mechanism of chitosan cross-linking with glutaraldehyde, Russ. J. Bioorg. Chem., 35 (2009) 360–369.
[44] M.C. Dartiguenave, M.J. Bertrand, K.C. Waldron, Glutaraldehyde: behavior in aqueous solution, reaction with proteins, and application to enzyme crosslinking, Biotechniques, 37 (2004) 790–802.
[45] R. Huang, B. Yang, Q. Liu, Removal of chromium(VI) ions from aqueous solutions with protonated crosslinked chitosan, J. Appl. Polym. Sci., 129 (2013) 908–915.
[46] O.A.C. Monterio Jr., C. Airoldi, Some studies of crosslinking chitosan-glutaraldehyde interaction in a homogeneous system, Int. J. Biol. Macromol., 26 (1999) 119–128.
[47] D. Liu, C. Poon, K. Lu, C. He, W. Lin, Self-assembled nanoscale coordination polymers with trigger release properties for effective anticancer therapy, Nat. Commun., 5 (2014) 4182–4192.
[48] S.J. Lim, J.H. Lee, M.G. Piao, M.K. Lee, D.H. Oh, H. Hwang du, Q.Z. Quan, C.S. Yong, H.G. Choi, Effect of sodium carboxymethylcellulose and fucidic acid on the gel characterization of polyvinylalcohol-based wound dressing, Arch. Pharm. Res., 33 (2010) 1073–1081.
[49] K. Dusek, W. Prins, Structure and elasticity of non-crystalline polymer networks, Adv. Polym. Sci., 6 (1969) 1–102.
[50] M. Zhang, Y. Liu, T. Li, W. Xu, B. Zheng, X. Tan, H. Wang, Y. Guo, F. Guo, S. Wang, Chitosan modification of magnetic biochar produced from *Eichhornia crassipes* for enhanced sorption of Cr(VI) from aqueous solution, RSC Adv., 5 (2015) 46955–46964.
[51] N. Lapa, R. Barbosa, M.H. Lopes, B. Mendes, P. Abelha, I. Gulyurtlu, J.S. Oliveira, Chemical and ecotoxicological characterization of ashes obtained from sewage sludge combustion in a fluidised-bed reactor, J. Hazard. Mater., 147 (2007) 175–183.
[52] H. Li, Z. Li, T. Liu, X. Xiao, Z. Peng, L. Deng, A novel technology for biosorption and recovery hexavalent chromium in wastewater by bio-functional magnetic beads, Bioresour. Technol., 99 (2008) 6271–6279.
[53] M. Kumar, B.P. Tripathi, V.K. Shahi, Crosslinked chitosan/polyvinyl alcohol blend beads for removal and recovery of Cd(II) from wastewater, J. Hazard. Mater., 172 (2009) 1041–1048.
[54] Y. Jiang, X. Yu, T. Luo, Y. Jia, J. Liu, X. Huang, γ-Fe_2O_3 nanoparticles encapsulated millimeter-sized magnetic chitosan beads for removal of Cr(VI) from water: thermodynamics, kinetics, regeneration, and uptake mechanisms, J. Chem. Eng. Data, 58 (2013) 3142–3149.
[55] D. Xu, K. Zhu., X. Zheng, R. Xiao, Poly(ethylene-co-vinyl alcohol) functional nanofiber membranes for the removal of Cr(VI) from water, Ind. Eng. Chem. Res., 54 (2015) 6836–6844.
[56] Y.A. Aydin, N.D. Aksoy, Adsorption of chromium on chitosan: optimization, kinetics and thermodynamics, Chem. Eng. J., 151 (2009) 188–194.
[57] S. Hena, Removal of chromium hexavalent ion from aqueous solutions using biopolymer chitosan coated with poly 3-methyl thiophene polymer, J. Hazard. Mater., 181 (2010) 474–479.
[58] S. Karahan, M. Yurdakoc, Y. Seki, K. Yurdakoc, Removal of boron from aqueous solution by clays and modified clays, J. Colloid Interface Sci., 293 (2006) 36–42.
[59] G. Bayramoglu, M.Y. Arica, Adsorption of Cr(VI) onto PEI immobilized acrylate-based magnetic beads: isotherms, kinetics and thermodynamics study, Chem. Eng. J., 139 (2008) 20–28.
[60] Y. Lu, B. Jiang, L. Fang, F. Ling, J. Gao, F. Wu, X. Zhang, High performance NiFe layered double hydroxide for methyl orange dye and Cr(VI) adsorption, Chemosphere, 152 (2016) 415–422.
[61] L. Zhang, W. Xia, X. Liu, W. Zhang, Synthesis of titanium cross-linked chitosan composite for efficient adsorption and detoxification of hexavalent chromium from water, J. Mater. Chem., 3 (2015) 331–340.
[62] J. Ananpattarachai, P. Kajitvichyanukul, Enhancement of chromium removal efficiency on adsorption and photocatalytic reduction using a bio-catalyst, titania-impregnated chitosan/xylan hybrid film, J. Clean. Prod., 130 (2016) 126–136.
[63] L. Sun, L. Zhang, C. Liang, Z. Yuan, Y. Zhang, W. Xu, J. Zhang, Y. Chen, Chitosan modified Fe^0 nanowires in porous anodic alumina and their application for the removal of hexavalent chromium from water, J. Mater. Chem., 21 (2011) 5877–5880.
[64] L. Luo, W. Cai, J. Zhou, Y. Li, Facile synthesis of boehmite/PVA composite membrane with enhanced adsorption performance towards Cr(VI), J. Hazard. Mater., 318 (2016) 452–459.
[65] H. Ren, Z. Gao, D. Wu, J. Jiang, Y. Sun, C. Luo, Efficient Pb(II) removal using sodium alginate-carboxymethyl cellulose gel beads: preparation, characterization, and adsorption mechanism, Carbohydr. Polym., 137 (2016) 402–409.
[66] B. Jiang, J. Guo, Z. Wang, X. Zheng, J. Zheng, W. Wu, M. Wu, Q. Xue, A green approach towards simultaneous remediations of chromium(VI) and arsenic(III) in aqueous solution, Chem. Eng. J., 262 (2015) 1144–1151.